Author(s): Barmparis, Georgios D.; Honkala, Karoliina; Remediakis, Ioannis N.

Title: Thiolate Adsorption on Au(hkl) and Equilibrium Shape of Large Thiolate-covered Gold Nanoparticles

Year: 2013

Version:

Please cite the original version:

Barmparis, G. D., Honkala, K., & Remediakis, I. N. (2013). Thiolate Adsorption on Au(hkl) and Equilibrium Shape of Large Thiolate-covered Gold Nanoparticles. Journal of Chemical Physics, 138(6), 064702/9. https://doi.org/10.1063/1.4790368

Thiolate adsorption on Au(hkl) and equilibrium shape of large thiolate-covered gold nanoparticles

Georgios D. Barmparis, Karoliina Honkala, and Ioannis N. Remediakis

Citation: The Journal of Chemical Physics **138**, 064702 (2013); doi: 10.1063/1.4790368
View online: http://dx.doi.org/10.1063/1.4790368
View Table of Contents: http://scitation.aip.org/content/aip/journal/jcp/138/6?ver=pdfcov
Published by the AIP Publishing

Thiolate adsorption on Au(hkl) and equilibrium shape of large thiolate-covered gold nanoparticles

Georgios D. Barmparis,[1,a)] Karoliina Honkala,[2] and Ioannis N. Remediakis[1]
[1]*Department of Materials Science and Technology, University of Crete, Heraklion, 71003 Crete, Greece*
[2]*Department of Chemistry, Nanoscience Center, University of Jyväskylä, P.O. Box 35, 40014 Jyväskylä, Finland*

(Received 3 August 2012; accepted 22 January 2013; published online 8 February 2013)

The adsorption of thiolates on Au surfaces employing density-functional-theory calculations has been studied. The dissociative chemisorption of dimethyl disulfide (CH_3S-SCH_3) on 14 different Au(hkl) is used as a model system. We discuss trends on adsorption energies, bond lengths, and bond angles as the surface structure changes, considering every possible Au(hkl) with h, k, $l \leq 3$ plus the kinked Au(421). Methanethiolate (CH_3S-) prefers adsorption on bridge sites on all surfaces considered; hollow and on top sites are highly unfavourable. The interface tensions for Au(hkl)-thiolate interfaces is determined at low coverage. Using the interface tensions in a Wulff construction method, we construct atomistic models for the equilibrium shape of large thiolate-covered gold nanoparticles. Gold atoms in a nanoparticle change their equilibrium positions upon adsorption of thiolates towards shapes of higher sphericity and higher concentration of step-edge atoms. © *2013 American Institute of Physics*. [http://dx.doi.org/10.1063/1.4790368]

I. INTRODUCTION

Understanding the nature of interactions between metals and soft or hard condensed matter systems is a crucial step in the design of new nanocomposite materials. In particular, understanding the factors that affect the shape and size of metal nanoparticles during growth might trigger a new generation of experiments based on the controlled synthesis of nanoparticle-based materials for various applications, including ultra-hard coatings, catalysts of high selectivity, fine-tuned optoelectronic devises, or smart materials for drug delivery and other biomedical applications. During the past two decades, the formation and structure of self-assembled monolayers (SAMs) of alkanethiol molecules adsorbed at noble materials' surfaces has attracted great interest.[1] Especially gold nanoparticles have been used in a variety of applications in biology, catalysis, and nanotechnology.[2] The interface between alkanethiols and gold is, therefore, a subject of great importance for both basic and applied research. The fundamental question is of course the type and strength of the Au–S bonds at this interface.

There are many theoretical Density-Functional-Theory (DFT) studies on the adsorption of alkanethiols on Au(111). The majority of them investigates the adsorption energy of CH_3S- radical on Au(111).[3–12] Various groups have studied the dissociative adsorption of dimethyl disulfide (DMDS) on Au(111), both theoretically[3,11] and experimentally.[13–15] In particular, Nuzzo *et al.*[13] suggested, after employing a large variety of experimental methods including X-ray photoelectron spectroscopy (XPS), Auger electron spectroscopy (AES), high-resolution electron energy loss spectroscopy (HREELS), and thermal desorption spectroscopy (TDS), that the breaking of the (weak) S–S bond of DMDS leads to the formation of two methanethiolate-surface bonds on Au(111) at low coverage. This cleavage is known to take place even at room temperature.[15] The adsorption of a CH_3S- radical has also been studied on Au(100) and Au(110) surfaces by Masens *et al.*[9] who found that the adsorption energy of CH_3S- on Au(110) is lower by 0.13 eV than that on (100) and by about 0.43 eV than that of (111). Despite the large number of theoretical studies the nature of a binding site is an open issue. In addition, a systematic study of the adsorption of a CH_3S- radical and the dissociative adsorption of DMDS on high index gold surfaces is missing.

The interaction between alkanethiols and gold has also been studied through several theoretical works on thiolate-protected gold clusters, either using DFT simulations[16–19] or Molecular Dynamics (MD) simulations[20] to explore the structure and electronic properties of such clusters. In these studies, it was found that the structure and electronic properties of the gold core of ligand-capped gold nanoclusters depend on the chemical nature of the ligand.

For most studies regarding small Au clusters, it has been found that thiolates heavily change the surface structure, by creating Au adatoms. Each Au adatom is bonded to two thiolates, and each terminal S atom makes two bonds, one with the Au adatom and another one with a surface Au atom. This bond has been found to be extremely stable for small Au clusters.[19,21,22] The same configuration, including Au adatoms bonded to two RS- groups, has been named the "standard model" for close-packed methylthiolate self-assembled monolayers on Au(111),[23] as it has been found in several experimental and theoretical studies for this system.[24–27] Such bonds between two S atoms and a Au adatom appear due to low reactivity of Au atoms in the close-packed (111) surface, and are expected to be less likely in stepped or kinked surfaces, where undercoordinated Au atoms form significantly stronger bonds to S. Moreover, the strong steric repulsions

a)Electronic mail: barmparis@materials.uoc.gr.

associated with adsorption of longer molecules will result in grafting densities of the order of 1 nm^{-2} or less,[28] where it is unlikely that thiolate groups from two different molecules will bind to the same Au atom.

Computational studies of thiolate-protected nanoparticles are usually limited to clusters that generally contain at most a few hundred Au atoms. To investigate the shape of larger thiolate-covered gold nanoparticles, one can use the Wulff construction which has been routinely employed in modern theoretical nanoscience. Examples include Ru nanoparticles for NH_3 synthesis,[29] Cu nanoparticles in catalysis,[30] and strained semiconductor quantum dots.[31] Recently, the Wulff construction has been employed to predict the shape of a nanoparticle when interactions between a nanoparticle and its environment are included.[32–39]

In the present study, we performed DFT calculations to investigate the dissociative adsorption of dimethyl disulfide (CH_3S–SCH_3) on Au(*hkl*) surfaces with $h, k, l \leq 3$, and on the kinked Au(421) surface at low-coverage. Furthermore, adsorption energies were employed to calculate interfacial tension between CH_3S and Au(*hkl*) surfaces. Using the Wulff construction method, we predict the equilibrium shape of thiolate-protected gold nanoparticles.

The paper is organized as follows: Section II describes computational details, the definition of the adsorption energy, and introduces the concept of the equilibrium shape. In Sec. III, we discuss the adsorption of CH_3S on Au surfaces together with the adsorption energies of various adsorption sites for each surfaces. In Sec. IV, the effects of dimethyl disulfide environment on gold nanoparticles are presented and finally the obtained results are summarized in Sec. V.

II. METHODOLOGY

A. Adsorption

To save computer time, only the simplest possible alkanethiol radical, methanethiolate (RS- with R=CH_3) is considered. Although this excludes steric repulsions between chains, it captures all essential features of the general RS–Au bond. This is a reasonable choice as shown by the recent work of Torres *et al.*[40] These authors show that the adsorption energy of n-alkanethiols on Au(111) changes by only 2 kcal/mol (0.09 eV/molecule) when the length of chain increases from one to six carbon atoms. Steric interactions between chains have a minor impact on binding energies; for example, Torres *et al.*[40] find that the binding energies of ethanethiolate and propanethiolate are affected by chain interactions by only 0.1 kcal/mol and 0.7 kcal/mol, respectively.

Our second choice is to focus on low coverage of RS on Au, corresponding to coverages less than 0.2 ML, where the adsorption energy is independent of coverage according to our simulation model. For most cases, the grafting density of adsorbates is of the order of 1 nm^{-2}, in accordance with Au nanoparticles dispersed in polymer matrices.[28] In this region, interactions between adsorbates can be neglected and the dissociative adsorption energy of dimethyl disulfide on Au(*hkl*) per methanethiolate, E_{ads} can be defined as

$$E_{ads} = E^{slab}_{\mathrm{Au}(hkl)\mathrm{SCH_3}} - E^{slab}_{\mathrm{Au}(hkl)} - \frac{1}{2}E^{(gas)}_{\mathrm{CH_3SSCH_3}}, \quad (1)$$

where $E^{slab}_{\mathrm{Au}(hkl)-\mathrm{SCH_3}}$ is the total energy of thiolate-covered slab, $E^{slab}_{\mathrm{Au}(hkl)}$ is the total energy of the clean slab, and $E^{(gas)}_{\mathrm{CH_3SSCH_3}}$ the energy of dimethyl disulfide in gas phase.

B. Computational details

First-principles total energy calculations were performed using DFT as it is implemented in the GPAW/ASE code[41,42] (https://wiki.fysik.dtu.dk). GPAW uses a projector-augmented wave method to describe core electrons, and it employs real space grids to present electron densities and wave functions. We applied grid spacing of 0.19 Å, and the Brillouin zone of the (111)–(1×1) surface was modelled by a (10×10×1) Monkhorst-Pack grid of $\vec{k}$-points. $\vec{k}$-points for all other surfaces are calculated in proportionality to the (111)–(1×1) slab ones. Periodic boundary conditions were applied in all three dimensions. Slabs had thickness of 8 Å or more and they were separated by 12 Å of vacuum. Slab thickness was chosen so that adsorption energy for few characteristic (*hkl*) orientations was converged within 10 meV. The positions of all adsorbate atoms as well as the first two layers of the slab were fully relaxed. We applied the generalized gradient approximation (GGA) revised Perdew-Burke-Ernzerhof exchange-correlation functional (RPBE). The theoretical lattice constant for Au (4.22 Å) was used, which was found by minimizing the total energy of bulk Au. The slight overestimation of the lattice constant compared to experimental value 4.08 Å is consistent with previous DFT calculations.[43] As we are interested in low thiolate coverage, we make sure that the unit cells are large enough. The minimum distance between an S atom and its periodic image is 5 Å or more in all cases. Thus, it is expected that interaction between adjacent molecules is negligible. Calculations for the gas phase dimethyl disulfide molecule were carried out in a (16×16×16) $Å^3$ unit cell so that interactions between periodically repeated molecules are negligible. Figure 1 displays some typical adsorption overlayer structures investigated in the present study.

C. Equilibrium shape

Under thermodynamic equilibrium, the shape of a given quantity of condensed matter, is that with the minimum total surface energy. In 1901, mineralogist G. Wulff proposed that the closed shape that minimizes the total surface energy is such that the distance of each face from the center (center of mass), d_{hkl} is proportional to the surface tension γ_{hkl} of the respective surface,[44]

$$d_{hkl} \sim \gamma_{hkl}. \quad (2)$$

For simplicity, we extend the use of the term "surface tension" for solids, as a synonym for surface energy per unit area. From this equation, it is easy to show that the distance, d_{hkl}, for any

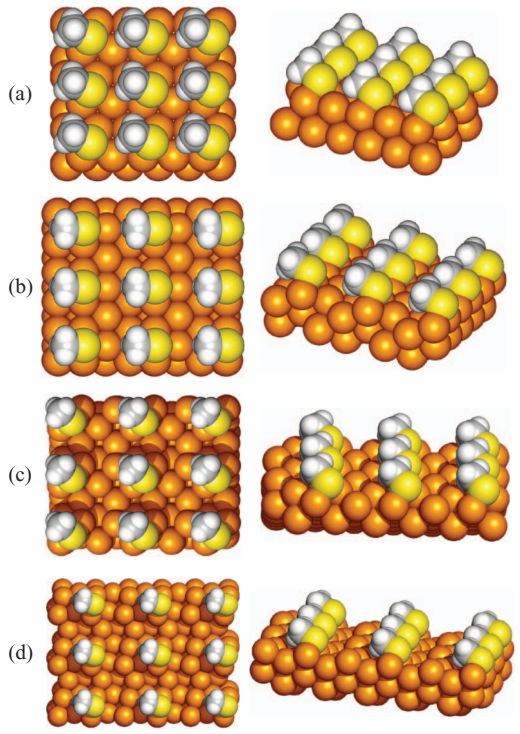

FIG. 1. Top (left) and side (right) view of thiolate-covered Au surfaces. (a) Au(111), (b) Au(211), (c) Au(310), and (d) Au(421). A (3 × 3) repetition of the simulation cell is shown.

face (*hkl*) is given by

$$d_{hkl} = d_{h'k'l'} \frac{\gamma_{hkl}}{\gamma_{h'k'l'}}, \tag{3}$$

where γ_{hkl} and the $\gamma_{h'k'l'}$, are the surface tensions of the (*hkl*) and ($h'k'l'$) surfaces, respectively, and $d_{h'k'l'}$ is the distance of the ($h'k'l'$) face. The latter determines the size of the nanoparticle. Equation (3) is the general equation to calculate the distance of the faces of a closed shape nanoparticle given the surface tension for each surface.

A Wulff construction based on a large set of (*hkl*) surfaces should, in principle, account for various kinds of surface defects, including steps, kinks, or even adatoms for large enough nanoparticles. These defects can be described by a suitable (*hkl*) surface. For example, a vicinal fcc(111) surface, where (111) terraces are separated by monoatomic steps are described by the (*hkk*) family of surfaces. The point where four such surfaces meet is represented by an adatom on a hollow site of fcc(111) (compare, for example, Figs. 3 and 4).

When the nanoparticle interacts with the surrounding environment, the surface tension is replaced by the tension of the interface between the nanoparticle faces and the environment, i.e., the interfacial tension. The interfacial tension, γ_{int}, depends on the surface tension of the clean surface, γ, and the adsorption energy, E_{ads}, of the adsorbate to the nanoparticle faces. The interfacial tension can be obtained through DFT slab calculations. For a slab that contains N_{ad} adsorbated molecules in addition to its N atoms, is given by

$$\gamma_{int} = \gamma + \frac{N_{ad} E_{ads}}{A}, \tag{4}$$

where A is the area parallel to (*hkl*).[39]

Wulff construction is based on a simple geometrical criterion that the distance of each face is proportional to the surface tension. This favors low-index faces over high-index ones, as high-index faces are steeper. As an example, consider the equation of the (*hkl*) plane in the Wulff construction,

$$hx + ky + lz = d_{hkl}\sqrt{h^2 + k^2 + l^2}. \tag{5}$$

This plane intercepts the x axis at $x = d_{hkl}\sqrt{1 + (k/h)^2 + (l/h)^2}$, which clearly increases with increasing k and l. If two planes have the same surface tension, and hence the same distance, d_{hkl}, from the origin, planes with lower k and l indices will be closer to the origin along x axis and, therefore, will be more prominent in the Wulff construction around the x direction. Similar arguments apply to other directions, so that planes with high Miller indexes are underrepresented in the equilibrium shape. The Wulff construction method is correct at the thermodynamic limit of very large particles. Nevertheless, Wulff shapes for Au nanoparticles are found to agree with experimental observations even for nanoparticles that contain only a few hundreds of atoms.[39]

III. DISSOCIATIVE ADSORPTION OF CH_3S–SCH_3 ON GOLD SURFACES

The dissociative adsorption energy of dimethyl disulfide was calculated on Au(*hkl*) surfaces with h, k, $l \leq 3$ and Au(421). We considered several different adsorption sites and CH_3S configurations to ensure that the global minimum is found. The Au(*hkl*) surfaces with h, k, $l \leq 3$, can grouped into three categories: planar [(100), (110), and (111)], stepped [(210), (211), (221), (310), (311), (322), (331), and (332)] and kinked (321). Au(321) is the only kinked surface for h, k, $l \leq 3$. For this reason, we also simulated Au(421) to be sure that our results are applicable to at least two different kinked surfaces. The stepped surfaces can be further divided into subgroups according to the microfacet notation,[45] depending on the type of the terraces and step edges. In the microfacet notation, a surface with an n-atom wide (*hkl*) terrace separated by an ($h'k'l'$) step is denoted by n(*hkl*)×($h'k'l'$).[46]

In the following, we discuss briefly the main characteristics of each surface and the adsorption behaviour of methanethiolate on all of them. We consider at least three different adsorption sites for each surface, while more than ten different sites have been tested for the more complex systems. Some characteristic adsorption energies and geometrical details including adsorption site, metal-adsorbate bond lengths, and angles are summarized in Table I.

Au(100), Au(110), and Au(111): On all planar surfaces CH_3S prefers a bridge site, with exothermic adsorption energies of −0.57, −0.71, and −0.15 eV, respectively. The adsorption energy seems to be invariant under rotations of the methyl group around the S–C bond, since this rotation changes the adsorption energy only by a few meV. We find that E_{ads} is roughly inversely proportional to the coordination number, z, of Au atoms bonded to S: 8 for (100), 7 for (110), and 9 for (111). On-top and hollow adsorption sites are highly unfavourable. Adsorption of CH_3S on these sites is marginally exothermic or even endothermic. The only

TABLE I. Properties of methanethiolate adsorption on Au surfaces. A is the area per adsorbate in Å^2, and z is the average coordination number of the Au atoms bonded to S. The adsorption geometry is described by three letters: The first refers to the position of the sulfur atom: (t) for on top, (b) for bridge, and (h) for hollow. The second letter defines the orientation of the methyl group: (t) for planar surfaces, (u) for above the upper terrace, and (l) for above the lower terrace in stepped surfaces. The third letter refers to the direction of one hydrogen atom: (t) for towards the surface, (a) for away from the surface, and (p) when all hydrogen atoms are parallel to the surface. E_{ads} is the adsorption energy, $\phi_{\mathrm{Au-S-Au}}$ the angle between the S and the two Au atoms bonded to S for bridge and hollow site only, $\theta_{\mathrm{Au-S-C}}$ is the angle between the Au atom bonded to S, the S atom and the carbon. $d_{\mathrm{Au-S}}$ and $d_{\mathrm{S-C}}$ are the bond lengths between the Au and S atom and the S and C atom respectively.

Surface	Microfacet notation	A	z	Configuration	E_{ads} (eV)	$\phi_{\mathrm{Au-S-Au}}$ (deg)	$\theta_{\mathrm{Au-S-C}}$ (deg)	$d_{\mathrm{Au-S}}$ (Å)	$d_{\mathrm{S-C}}$ (Å)	Adsorption sites	Relaxed configuration
100	…	35.62	8.0	b-t-t	−0.57	79.7	110.1	2.46	1.85	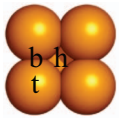	
				b-t-a	−0.52	79.6	108.7	2.47	1.85		
				h-t-p	−0.20	70.7	125.0	2.67	1.86		
				t-t-a	0.06	…	108.1	2.39	1.84		
110	…	37.78	7.0	b-t-a	−0.71	79.0	109.1	2.46	1.85	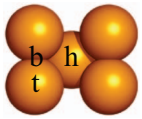	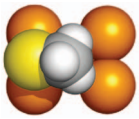
		50.37		b-t-a	−0.709	77.8	108.1	2.45	1.85		
		50.37		b-t-t	−0.708	78.6	105.1	2.44	1.84		
		50.37		t-t-t	−0.23	…	107.0	2.35	1.84		
111	…	30.85	9.0	b-t-a	−0.153	76.3	110.1	2.52	1.85	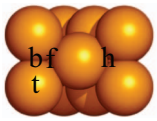	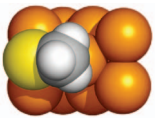
				b-t-t	−0.146	77.2	111.6	2.52	1.85		
				t-t-t	0.12	…	109.7	2.40	1.83		
				h-t-p	0.13	67.9	135.6	2.61	1.87		
310	3(100)×(110)	56.32	7.0	b-l-t	−0.59	84.9	109.0	2.45	1.85	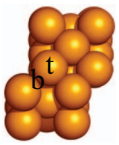	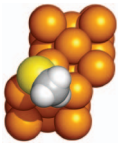
		28.16	7.0	b-l-t	−0.47	80.6	110.7	2.47	1.84		
		28.16	6.0	t-l-t	−0.22	…	108.7	2.34	1.83		
210	2(100)×(110) or 2(110)×(100)	59.73	7.5	b_1-u-t	−0.54	81.3	108.0	2.47	1.84	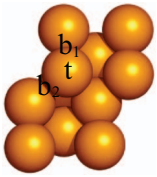	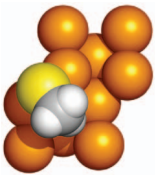
		59.73	7.5	b_2-u-t	−0.49	77.1	107.8	2.47	1.84		
		59.73	6.0	t-l-a	−0.28	…	106.3	2.34	1.83		
		39.82	6.0	t-l-a	−0.27	…	105.9	2.35	1.84		
320	3(110)×(100)	64.21	7.5	b_2-l-t	−0.511	81.8	109.2	2.46	1.84		
			6.5	b_1-u-a	−0.508	81.4	116.1	2.44	1.85		
			6.0	t-l-a	−0.24	…	105.4	2.34	1.83		
			6.0	t-l-t	−0.21	…	109.2	2.35	1.84		
311	2(100)×(111) or 2(111)×(100)	59.06	7.0	b-l-t	−0.75	81.1	106.2	2.43	1.84		
				b-l-a	−0.71	80.6	106.2	2.43	1.85		
211	3(111)×(100)	43.62	7.0	b-l-t	−0.75	80.6	106.6	2.44	1.84	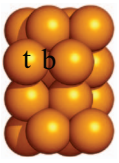	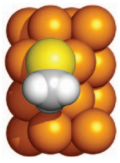
		43.62		b-l-a	−0.73	80.7	106.9	2.43	1.85		
		43.62		b-u-t	−0.72	80.0	105.1	2.44	1.85		
		43.62		t-l-a	−0.19	…	105.8	2.37	1.84		
		87.24		b-l-t	−0.81	85.3	107.4	2.45	1.84		
322	5(111)×(100)	73.43	7.0	b-l-t	−0.79	80.9	107.7	2.43	1.84		
				t-l-t	−0.17	…	106.8	2.35	1.84		

TABLE I. (*Continued.*)

Surface	Microfacet notation	A	z	Configuration	E_{ads} (eV)	$\phi_{Au-S-Au}$ (deg)	θ_{Au-S-C} (deg)	d_{Au-S} (Å)	d_{S-C} (Å)	Adsorption sites	Relaxed configuration
331	3(111)×(111)	77.63	7.0	b-l-t	−0.72	77.1	103.8	2.46	1.84		
				b-l-a	−0.69	76.5	105.3	2.46	1.84		
				b-u-a	−0.67	76.1	107.5	2.47	1.85		
221	4(111)×(111)	53.43	7.0	b-l-t	−0.68	76.3	107.5	2.47	1.84	t b	
				b-l-a	−0.64	75.8	108.4	2.47	1.85		
				t-l-t	−0.18	...	107.5	2.36	1.83		
332	6(111)×(111)	83.53	7.0	b-l-t	−0.64	77.3	107.2	2.46	1.84		
				t-l-t	−0.15	...	107.8	2.36	1.84		
321	...	99.95	7.0	b2-l-t	−0.75	80.9	106.6	2.45	1.84		
			7.0	b1-l-t	−0.66	78.0	106.3	2.47	1.84		
			6.0	t-l-t	−0.32	...	105.5	2.34	1.85		
421	...	81.61	6.5	b3-l-t	−0.79	83.0	106.6	2.44	1.84	b_1 b_2 b_3 t	
			7.0	b1-l-t	−0.65	75.9	106.8	2.47	1.84		

stable configuration for a hollow site is when the carbon atom resides above the S atom and the hydrogen atoms are placed in a plane parallel to the surface. This configuration is metastable and has the longest bond length between Au–S (>2.60 Å), the smallest angle between Au–S–Au (<71°) and the biggest θ_{Au-S-C} (>125°) angle; values that are far from the average ones, which are 2.46 Å, 79.9°, and 107.6°, respectively. On (110) and on other (*hkl*) surfaces, a hollow site results in numerical instabilities due to unrealistic charge distribution. To save computational time, we focused on adsorption over bridge sites for the most demanding high-index faces.

These findings agree with other works from the literature. To compare adsorption energies, one has to define the reference state of methanethiolate. Several groups have studied methanethiolate adsorption on Au(111) both experimentally[47] and theoretically.[3,5–10,47] In these studies, the following four reactions are considered:

a. dissociative adsorption of $CH_3S–SCH_3$,
b. adsorption of CH_3S radical,
c. dissociative adsorption of CH_3S-H, and
d. same as (c), but H is desorbed as H_2.

For Au(111), we find that CH_3S prefers bridge site with adsorption energies of (a) −0.15 eV, (b) −1.26 eV, (c) +0.91 eV, and (d) +0.32 eV. These results agree with the calculations of Molina and Hammer[8] who found −1.13 eV for (b) and +0.40 eV for (d). For (a), Hayashi *et al.*,[48] report a bridge site adsorption with −0.27 eV per CH_3S using the PBE exchange-correlation functional. Although the adsorption energy is different, there is good agreement for adsorption geometry. For example, the bond length between Au and S is 2.50 Å, very close to 2.52 Å found here. Andreoni *et al.*[3] find −1.60 eV for case (b) and −2.39 eV when PBE was used, confirming that PBE overestimates Au–S binding. They report the Au–S bond at 2.46 Å. Similarly, Maksymovych *et al.*[47] found a binding energy of −1.77 eV for (b) and a bond length of 2.45 Å for the same adsorption geometry. Masens *et al.*[9] report an adsorption energy of −1.70 eV for (b) close to −1.73 eV found by Yourdshahyan *et al.*[5] In case (c), Zhou and Hagelberg[10] report a dissociative adsorption energy of −0.06 eV, but they conclude that the adsorption of the methanethiol is nondissociative since the nondissociative structure of methanthiol displays a higher adsorption energy than the dissociative one by 0.6 eV. They also found the Au–S bond length to be 2.45 Å. The nondissociative adsorption of $CH_3S–H$ has been observed experimentally by Maksymovych *et al.*[47] using scanning tunneling microscopy (STM).

The difference between adsorption energies for (110) or (100) and (111) is found to be 0.14 eV and 0.42 eV, respectively. These values are in excellent agreement to 0.13 eV and 0.43 eV, respectively, reported by Masens *et al.*[9]

Having established the validity of our method for planar surfaces where several experiments and simulations have been reported, we now proceed to the study of thiolate adsorption on stepped and kinked Au surfaces.

Au(210), Au(310), and Au(320): According to the stereographic triangle[46] of the fcc system, these three stepped surfaces coexist along the same direction, travelling from the (100) to the (110) corner. Hence, (310) can be referred as 3(100)×(110), while (210) is on the so called turning point of the zone, where steps and terraces are indistinguishable, and can be referred to both as 2(100)×(110) and 2(110)×(100). (320) consists of 3-atoms wide (110) terrace and (100)-like step. On (310), CH_3S prefers a bridge site between a step-edge and a step-bottom atom, with coordination number 7 and adsorption energy −0.59 eV. On (210) and (320), the most stable configurations found for two bridge sites, one between

a step-edge and a step-bottom atom and one between a step-edge and a terrace atom, both with average coordination number $z = 7.5$. The difference between the adsorption energies is less than 0.05 eV. The adsorption energy for the most stable of them is −0.54 eV for (210) and −0.51 eV for (320). In all cases, the on-top site was found to have less exothermic adsorption energy by about 0.30 eV.

Au(211), Au(311), and Au(322): (311) is a surface on the turning point of the stereographic triangle and thus can be referred as a 2-atoms wide (100) terrace separated by (111)-like step or 2-atoms wide (111) terrace separated by (100)-like step. It has step-edge atoms with $z = 7$ and step-bottom atoms with $z = 10$. (211) and (311) are referred to as 3-atoms and 5-atoms wide (111) terrace and (100)-like step, respectively. Au(211) is a typical stepped Au surface, and we commenced our study with this system. We considered about 15 different adsorption configurations to ensure that all low-energy adsorption geometries are taken into account. The preferred one is a bridge site between two step-edge atoms with $z = 7$ each, having the methyl group above the lowest terrace and the hydrogen atoms in such a way that one hydrogen is towards the lower terrace and the other two away from it. The adsorption energy for this configuration is −0.75 eV. There are also two metastable states. One with the methyl group rotated along the S–C bond, having two hydrogen atoms towards the lower terrace and one away from it, with $E_{ads} = -0.73$ eV and an other one with the methyl group above the upper terrace with $E_{ads} = -0.72$ eV. The hollow site was found to be highly unfavourable. That it finally relaxed to a step-bridge site. The adsorption energy changes only by 60 meV upon doubling the area of the unit cell, proving that at low-coverage the adsorption energy is independent of the coverage.

Au(221), Au(331), and Au(332): These three surfaces consist of 3-, 4-, and 6-atoms wide (111) terraces, respectively, separated by (111)-like step edge. The step-edge atoms have 7 neighbours, the terrace atoms 9, and the step-bottom ones have 11. The adsorption energy is −0.72, −0.68, and −0.64 eV, respectively, for a bridge site with the S atom between two step-edge atoms and the methyl group above the lower terrace. Bond lengths of Au−S and S−C and the angles $\phi_{\mathrm{Au-S-Au}}$ and $\theta_{\mathrm{Au-S-C}}$ are very close to the average values.

Au(321) and Au(421): These are kinked surfaces, i.e., contain regular nonlinear steps. The step edge of (321) consists of 2-atoms wide (100) and 2-atoms wide (111). The step-edge atoms have 6 or 8 neighbours alternately. The CH_3S binds on a bridge site between two atoms with 6 and 8 neighbours, with −0.75 eV energy. The step edge of (421) consists of 3-atoms wide (100) [one atom wired than (321)] and 2-atoms wide (111). The step-edge atoms have 6, 7, and 8 neighbours alternately. The CH_3S binds on a bridge site between two atoms with 6 and 7 neighbours, with $E_{ads} = -0.79$ eV. In both cases, the (111) terrace consists of atoms with 9 neighbours terminated by step-bottom atoms with 10 or 11 neighbours. Here, also, bond lengths of Au−S and S−C and the angles $\phi_{\mathrm{Au-S-Au}}$ and $\theta_{\mathrm{Au-S-C}}$ are very close to the total averages.

It is well established that E_{ads} for O and CO adsorption on Au is a linear function of the coordination number, z, of Au atoms.[39,49,50] To investigate whether this trend also holds for thiolates, we plot in Fig. 2 the adsorption energy as a function of z. Although a general trend for increase of E_{ads} with increasing z can be deduced from Fig. 2, a clear linear dependence was not found. Nevertheless, the average adsorption energies for each z can be fitted nicely to a straight line. Apparently, the CH_3S−Au bond depends on many parameters, and not just the coordination number. For example, such a parameter could be the d-band center of the surfaces. However, the *d*-band model is not readily applicable to Au surfaces, as Au atoms have filled *d* shells. Indeed, our calculations show little correlation between the center of the *d*-band and methanethiol adsorption energy. For comparison, a linear dependence between these two quantities has been established for a multitude of other systems.[51] To get a qualitative description of bonding to Au, one needs to apply the more general Newns-Anderson model. Larsen *et al.*[52] used this general theory to explain calculated adsorption energies of H, O, Li, and F on small Au clusters. However, adsorption of larger molecules, such as thiolates, is more complicated. In this case, electrons can be transferred not only around the adsorbate-metal bond but also in other parts of the molecule. It would have been very difficult to gain insight into this problem without using detailed density-functional theory simulations.

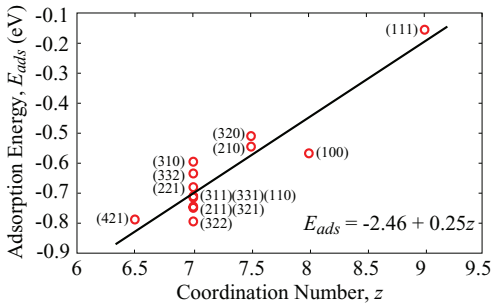

FIG. 2. Dissociative adsorption energy of CH_3S-SCH_3 on Au(*hkl*) as a function of the Au coordination number, z, and its linear fit.

Thiolates prefer bridge sites in all cases. In particular, for Au(111) our minimum energy adsorption geometry is identical to that presented by Hayashi *et al.*[48] and by Maksymovych *et al.*[47] The on top site was found to be the most unfavourable one, followed by the hollow site. In all stepped surfaces, the methyl part is oriented above steps and in all cases in such a way that one of the hydrogen atoms is directed towards the surface, whereas the other two are pointing away from the surface. The dissociative adsorption energy per thiolate E_{ads} ranges from −0.15 to −0.80 eV. The bond length Au−S was found to be (2.46 ± 0.02) Å, in agreement with experimental values (2.42 ± 0.03) Å from Ref. 14 and 2.48 Å from Ref. 53 and theoretical studies between 2.46 and 2.50 Å.[6,9,11,12,47,48] The angle $\phi_{\mathrm{Au-S-Au}}$ was found to be (79.9 ± 2.6)° and the angle $\theta_{\mathrm{Au-S-C}}$ (107.6 ± 1.7)°, very close to the tetrahedral structure with 109.5° that dimethyl disulfide prefers and in good agreement with 109.7° found in Ref. 47. In all cases, the distance between the sulfur and carbon atom was found to be about 1.84 Å in excellent agreement with 1.83 Å in Ref. 47 and 1.87 Å found in Ref. 4. The lowest absolute value for the adsorption energy (0.15 eV) is found for the

TABLE II. Ratios of the surface tension of an Au(*hkl*) surface with respect to the Au(211) surface tension, for covered with CH_3S and clean surfaces.

	CH_3S	Clean[a]
γ_{211} (J/m^2)	0.53	0.81
$\gamma_{100}/\gamma_{211}$	1.18	1.05
$\gamma_{110}/\gamma_{211}$	1.24	1.10
$\gamma_{111}/\gamma_{211}$	1.14	0.85
$\gamma_{210}/\gamma_{211}$	1.45	1.13
$\gamma_{310}/\gamma_{211}$	1.39	1.12
$\gamma_{311}/\gamma_{211}$	1.25	1.07
$\gamma_{320}/\gamma_{211}$	1.52	1.15
$\gamma_{321}/\gamma_{211}$	1.40	1.07
$\gamma_{322}/\gamma_{211}$	1.10	0.94
$\gamma_{331}/\gamma_{211}$	1.26	1.00
$\gamma_{332}/\gamma_{211}$	1.16	0.92

[a]Reference 39.

close-packed (111) surface. On this surface, we also find the longest Au−S distance (2.52 Å).

IV. THIOLATE-COVERED GOLD NANOPARTICLES

Having calculated the adsorption energies, we now use Eq. (4), together with Au(*hkl*) surface tension from Ref. 39, to calculate the interfacial tensions of thiolate-covered gold surfaces. Using Eq. (3) with a given distance for the $(h'k'l')$ surface, we find the distance for the other faces. We choose $(h'k'l')$ to be the (211) surface which is the one with the minimum interfacial tension. This minimum interfacial tension is a result of the highest absolute value for the adsorption energy combined with a high density of steps. In Table II, we present the ratios of the surface tension of an Au(*hkl*) surface with respect to the Au(211) surface tension, for covered with CH_3S and clean surfaces.

By increasing the d_{211} distance, we construct nanoparticles of increasing diameter. For each one of them we find all d_{hkl} and thus construct the Wulff polyhedron. Then we fill it with atoms in the fcc lattice and create an atomistic model of a nanoparticle. Two orthogonal unit cell bases for the fcc lattice of gold are used, one with an atom in the center and an other one without. We constructed more than 30 000 nanoparticles with diameters up to 40 nm. Only a few thousands of them are unique and less than a hundred are in agreement with the continuous Wulff polyhedron.

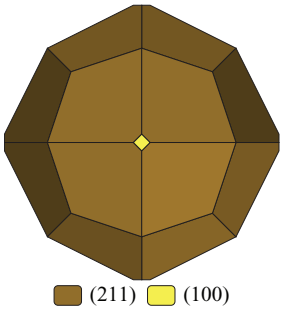

FIG. 3. Wulff construction for a thiolate-protected Au nanoparticle. The shape consists almost entirely of (211) faces.

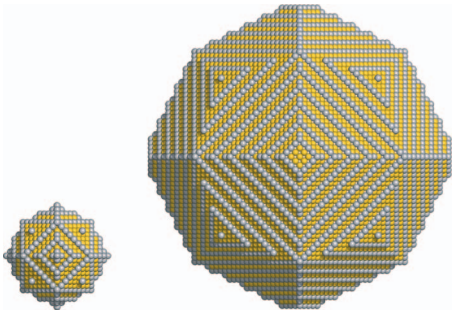

FIG. 4. Atomistic Wulff construction for thiolate-covered gold nanoparticles at 5.0 and 14.2 nm, respectively. Grey atoms are Au atoms at edges or corners.

The thus constructed shape might deviate from the thermodynamic limit at small sizes, as some faces might be too small to accommodate a unit cell. At the thermodynamic limit, thiolate-protected gold nanoparticles are almost totally dominated by the (211) surface with a very small amount of (100). In Fig. 3, the equilibrium shape at the thermodynamic limit is shown. This shape is close to a deltoidal icositetrahedron. In Fig. 4, we present atomistic models of the Wulff construction for two different sizes. The nanoparticle with diameter of 14.2 nm is identical to that at the thermodynamic limit. Smaller nanoparticles do not have (100) faces, as this area is smaller than the minimum unit cell of (100). This is the case for all nanoparticles smaller than 14.2 nm. In Table III, we present characteristic values for the nanoparticles in equilibrium, including diameter d in nm, number of the atoms in corners N_c, edges N_e, surfaces N_s, and total N_t. We also present the surface area in nm^2, the volume in nm^3, the active site density N_{act} in μmol/g assuming that step-edge atoms are active and the faces appearing for each nanoparticle with the percentages due to the total area for each one face.

Although our method is valid for large nanoparticles and for low coverage, nanoparticles shown in Fig. 4 compare very well to state-of-the-art simulations of the Au_{102}(p-MBA)$_{44}$ cluster by Walter *et al.*[17] In that work, a very high coverage is considered and Au adatoms bonded to two S atoms are present. When comparing the Au core (Au atoms except the adatoms), as depicted in Fig. 1 of Ref. 17, we find a surprising similarity: In both cases, Au atoms form three-atom-wide (111)-like terraces which are separated by monoatomic steps.

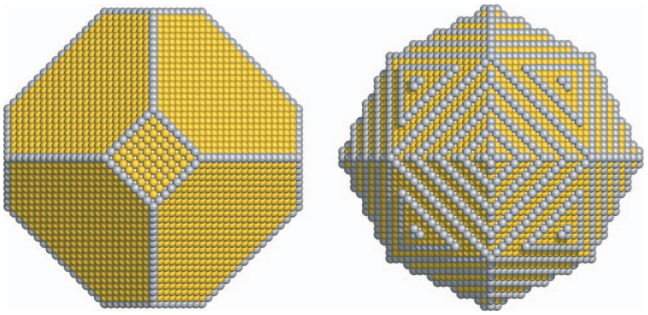

FIG. 5. (Left) Model of a typical Au nanoparticle (d ∼ 10 nm, ca. 22750 atoms) in non-interacting environment (sphericity = 89%, 78 μmol of active sites per g) (Right) a same size thiolate-protected gold nanoparticle (sphericity = 95%, 299 μmol of active sites per g). Step and kink atoms are shown in darker color.

TABLE III. Characteristic values for the stable nanoparticles, including diameter, d, of the Au core in nm, number of the atoms in corners N_c, edges N_e, surfaces N_s, and total N_t, the surface area in nm^2, the volume in nm^3, the active (step) site density N_{act} in μmol/g, and the faces appearing for each nanoparticle with the percentages due to the total area for each one face.

d (nm)	N_c	N_e	N_s	N_t	Area (nm^2)	Volume (nm^3)	N_{act} (μmol/g)	Faces
5.02	26	312	456	2461	62	42	644	(211) (100%)
10.45	60	1344	2352	22798	278	404	299	(211) (100%)
14.21	44	2664	4830	63511	553	1135	211	(211) (98.5%) (100) (1.5%)
19.23	44	4728	8742	149779	984	2691	159	(211) (99.1%) (100) (0.9%)
24.24	44	7368	13806	291631	1539	5257	127	(211) (99.5%) (100) (0.5%)
29.26	44	10584	20022	502891	2217	9086	106	(211) (99.6%) (100) (0.4%)
34.28	44	14376	27390	797383	3018	14428	91	(211) (99.7%) (100) (0.3%)

Comparing the shapes for gold core of thiolate-protected gold nanoparticles with gold nanoparticles in inert gas,[39] we find that the shape changes upon exposure to thiolates towards higher symmetry. An example is shown in Fig. 5. A gold nanoparticle with approximately 10 nm diameter, increases its sphericity from 89% in inert gas to 95%. The sphericity[54] of a nanoparticle equals $\pi^{1/3}(6V)^{2/3}/A$, where V is the volume and A is the area of it; characteristic values are 81% for a cube, 85% for an octahedron, and 100% for a sphere. Such shape change upon exposure to reactive environment is very common for Au nanoparticles.[39,55–57]

Thiolate-protected Au nanoparticles might be much more reactive compared to Au nanoparticles in weakly interacting environment. As a rough measure of activity, we consider the density of step-edge atoms. It has been found that undercoordinated Au atoms have increased chemical activity.[58,59] Of course, turnover for particular reactions will also depend on lateral interactions between adsorbates and thiolate species. In the case of very strong repulsive interactions, thiolate adsorption on Au might even result in decrease of Au reactivity. However, for reactions involving small molecules, such as CO oxidation, and for small thiolates at low coverage, such as those considered in this work, thiolate-protected Au is expected to be more reactive than a bare Au nanoparticle. Following the catalysis convention, we present in Table III the values of N_{act}, which is the number of μmol of active sites per g of material. This number can be of the order of 10^3 for nanoparticles of the order of 3 nm used in catalysis and drops down to 10^2 at diameters of a few tens of nm. Interestingly, for a nanoparticle of 10 nm N_{act} increases by a factor of 3.8 upon exposure to thiolates (see Fig. 5).

V. CONCLUSIONS

Adsorption of thiolates on 14 different Au(hkl) surfaces at very low coverage is studied as first step towards modelling encapsulated Au nanoparticle. A systematic study of adsorption of CH_3S on Au reveals that bridge sites are preferred in all cases. Several metastable configurations exist for each particular Au(hkl). Step edges show adsorption energies of -0.6 to -0.8 eV, while terraces have -0.5 eV or higher. Kinked sites do not show significantly stronger binding than step sites. The interface tension between Au(hkl) and thiolates at very low coverage has a strong dependence on the orientation of Au surface. Large thiolate-protected Au nanoparticles expose mostly (211) faces and are more spherical and more reactive than Au nanoparticles in weakly interacting matrices.

ACKNOWLEDGMENTS

Part of this work has been performed under the HPC-EUROPA2 project (Project No. hpce3116) with the support of the European Commission – Capacities Area – Research Infrastructures. The computer resources were provided by CSC the Finnish IT Center for Science, Espoo, Finland. We also acknowledge support by COST action MP0901 "nanoTP" and the Research Committee, University of Crete.

[1] C. Vericat, M. E. Vela, G. A. Benitez, J. A. M. Gago, X. Torrelles, and R. C. Salvarezza, J. Phys.: Condens. Matter **18**, R867 (2006).
[2] M.-C. Daniel and D. Astruc, Chem. Rev. **104**, 293 (2004).
[3] W. Andreoni, A. Curioni, and H. Grönbeck, Int. J. Quantum Chem. **80**, 598 (2000).
[4] Y. Akinaga, T. Nakajima, and K. Hirao, J. Chem. Phys. **114**, 8555 (2001).
[5] Y. Yourdshahyan, H. K. Zhang, and A. M. Rappe, Phys. Rev. B **63**, 081405 (2001).
[6] M. C. Vargas, P. Giannozzi, A. Selloni, and G. Scoles, J. Phys. Chem. B **105**, 9509 (2001).
[7] J. Gottschalck and B. Hammer, J. Chem. Phys. **116**, 784 (2002).
[8] L. M. Molina and B. Hammer, Chem. Phys. Lett. **360**, 264 (2002).
[9] C. Masens, M. J. Ford, and M. B. Cortie, Surf. Sci. **580**, 19 (2005).
[10] J.-G. Zhou and F. Hagelberg, Phys. Rev. Lett. **97**, 045505 (2006).
[11] H. Grönbeck, H. Häkkinen, and R. L. Whetten, J. Phys. Chem. C **112**, 15940 (2008).
[12] A. Franke and E. Pehlke, Phys. Rev. B **79**, 235441 (2009).
[13] R. G. Nuzzo, B. R. Zegarski, and L. H. Dubois, J. Am. Chem. Soc. **109**, 733 (1987).
[14] H. Kondoh, M. Iwasaki, T. Shimada, K. Amemiya, T. Yokoyama, T. Ohta, M. Shimomura, and S. Kono, Phys. Rev. Lett. **90**, 066102 (2003).
[15] M. G. Roper and R. G. Jones, Phys. Chem. Chem. Phys. **10**, 1336 (2008).
[16] H. Häkkinen, M. Walter, and H. Grönbeck, J. Phys. Chem. B **110**, 9927 (2006).
[17] M. Walter, J. Akola, O. Lopez-Acevedo, P. D. Jadzinsky, G. Calero, C. J. Ackerson, R. L. Whetten, H. Grönbeck, and H. Häkkinen, Proc. Natl. Acad. Sci. U.S.A. **105**, 9157 (2008).
[18] O. Lopez-Acevedo, J. Akola, R. L. Whetten, H. Grönbeck, and H. Häkkinen, J. Phys. Chem. C **113**, 5035 (2009).
[19] J. Akola, K. A. Kacprzak, O. Lopez-Acevedo, M. Walter, H. Grönbeck, and H. Häkkinen, J. Phys. Chem. C **114**, 15986 (2010).
[20] W. D. Luedtke and U. Landman, J. Phys. Chem. **100**, 13323 (1996).
[21] J. Akola, M. Walter, R. L. Whetten, H. Häkkinen, and H. Grönbeck, J. Am. Chem. Soc. **130**, 3756 (2008).
[22] D.-E. Jiang, M. Walter, and J. Akola, J. Phys. Chem. C **114**, 15883 (2010).
[23] H. Häkkinen, Nat. Chem. **4**, 443 (2012).
[24] P. Maksymovych, D. C. Sorescu, and J. T. Yates, Jr., Phys. Rev. Lett. **97**, 146103 (2006).

[25]R. Mazzarello, A. Cossaro, A. Verdini, R. Rousseau, L. Casalis, M. F. Danisman, L. Floreano, S. Scandolo, A. Morgante, and G. Scoles, Phys. Rev. Lett. **98**, 016102 (2007).
[26]A. Chaudhuri, M. Odelius, R. G. Jones, T. L. Lee, B. Detlefs, and D. P. Woodruff, J. Chem. Phys. **130**, 124708 (2009).
[27]O. Voznyy, J. J. Dubowski, J. T. Yates, and P. Maksymovych, J. Am. Chem. Soc. **131**, 12989 (2009).
[28]M. K. Corbierre, N. S. Cameron, and R. B. Lennox, Langmuir **20**, 2867 (2004).
[29]K. Honkala, A. Hellman, I. N. Remediakis, A. Logadottir, A. Carlsson, S. Dahl, C. Christensen, and J. K. Nørskov, Science **307**, 555 (2005); A. Hellman, K. Honkala, I. N. Remediakis, Á. Logadóttir, A. Carlsson, S. Dahl, C. H. Christensen, and J. K. Nørskov, Surf. Sci. **600**, 4264 (2006); **603**, 1731 (2009).
[30]B. S. Clausen, J. Schiøtz, L. Gråbæk, C. V. Ovesen, K. W. Jacobsen, J. K. Nørskov, and H. Topsøe, Top. Catal. **1**, 367 (1994); P. L. Hansen, J. B. Wagner, S. Helveg, J. R. Rostrup-Nielsen, B. S. Clausen, and H. Topsøe, Science **295**, 2053 (2002).
[31]P. Müller and R. Kern, Surf. Sci. **457**, 229 (2000).
[32]A. Barnard and P. Zapol, J. Chem. Phys. **121**, 4276 (2004).
[33]A. S. Barnard and L. A. Curtiss, Nano Lett. **5**, 1261 (2005).
[34]G. Hadjisavvas, I. N. Remediakis, and P. C. Kelires, Phys. Rev. B **74**, 165419 (2006).
[35]G. Kopidakis, I. N. Remediakis, M. G. Fyta, and P. C. Kelires, Diamond Relat. Mater. **16**, 1875 (2007).
[36]F. Mittendorfer, N. Seriani, O. Dubay, and G. Kresse, Phys. Rev. B **76**, 233413 (2007).
[37]A. Soon, L. Wong, B. Delley, and C. Stampfl, Phys. Rev. B **77**, 125423 (2008).
[38]H. Shi and C. Stampfl, Phys. Rev. B **77**, 094127 (2008).
[39]G. D. Barmparis and I. N. Remediakis, Phys. Rev. B **86**, 085457 (2012).
[40]E. Torres, A. T. Blumenau, and P. U. Biedermann, Chem. Phys. Chem. **12**, 999 (2011).
[41]J. J. Mortensen, L. B. Hansen, and K. W. Jacobsen, Phys. Rev. B **71**, 035109 (2005).
[42]S. R. Bahn and K. W. Jacobsen, Comput. Sci. Eng. **4**, 56 (2002).
[43]M. Fuchs, M. Bockstedte, E. Pehlke, and M. Scheffler, Phys. Rev. B **57**, 2134 (1998).
[44]C. Herring, Phys. Rev. **82**, 87 (1951).
[45]M. A. Van Hove and G. A. Somorjai, Surf. Sci. **92**, 489 (1980).
[46]G. Attard and C. Barnes, *Surfaces*, edited by R. G. Compton (Oxford University Press, 1998), Vol. 59.
[47]P. Maksymovych, D. C. Sorescu, and J. T. Yates, J. Phys. Chem. B **110**, 21161 (2006).
[48]T. Hayashi, Y. Morikawa, and H. Nozoye, J. Chem. Phys. **114**, 7615 (2001).
[49]N. Lopez and J. K. Nørskov, J. Am. Chem. Soc. **124**, 11262 (2002).
[50]G. Mpourmpakis, A. N. Andriotis, and D. G. Vlachos, Nano Lett. **10**, 1041 (2010).
[51]M. Mavrikakis, B. Hammer, and J. K. Nørskov, Phys. Rev. Lett. **81**, 2819 (1998).
[52]A. H. Larsen, J. Kleis, K. S. Thygesen, J. K. Nørskov, and K. W. Jacobsen, Phys. Rev. B **84**, 245429 (2011).
[53]M. Yu, N. Bovet, C. J. Satterley, S. Bengió, K. R. J. Lovelock, P. K. Milligan, R. G. Jones, D. P. Woodruff, and V. Dhanak, Phys. Rev. Lett. **97**, 166102 (2006).
[54]H. A. Wadell, J. Geol. **43**, 250 (1935).
[55]K. Ueda, T. Kawasaki, H. Hasegawa, T. Tanji, and M. Ichihashi, Surf. Interface Anal. **40**, 1725 (2008).
[56]K. P. McKenna, Phys. Chem. Chem. Phys. **11**, 4145 (2009).
[57]T. Uchiyama, H. Yoshida, Y. Kuwauchi, S. Ichikawa, S. Shimada, M. Haruta, and S. Takeda, Angew. Chem. Int., Ed. **50**, 10157 (2011).
[58]I. N. Remediakis, N. Lopez, and J. K. Nørskov, Angew. Chem. Int., Ed. **44**, 1824 (2005).
[59]H. Falsig, B. Hvolbæk, I. S. Kristensen, T. Jiang, T. Bligaard, C. H. Christensen, and J. K. Nørskov, Angew. Chem. Int., Ed. **47**, 4835 (2008).